Optomechanical Cavity With a Buckled Mirror

D. Yuvaraj, M. B. Kadam, Oleg Shtempluck, and Eyal Buks

***Abstract*—We study an optomechanical cavity, in which a buckled suspended beam serves as a mirror. The mechanical resonance frequency of the beam obtains a minimum value near the buckling temperature. Contrary to the common case, in which self-excited oscillations of the suspended mirror are optically induced by injecting blue detuned laser light, in our case, self-excited oscillations are observed with red detuned light. These observations are attributed to a retarded thermal (i.e., bolometric) force acting on the buckled mirror in the inward direction (i.e., toward the other mirror). With relatively high laser power, other interesting effects are observed, including period doubling of self-excited oscillations and intermode coupling. [2012-0198]**

***Index Terms*—Buckling, optomechanical cavity.**

I. Introduction

SYSTEMS combining mechanical elements in optical resonance cavities are currently a subject of intense interest [1]–[6]. Coupling of nanomechanical mirror resonators to optical modes of high-finesse cavities mediated by the radiation pressure has a promise of bringing the mechanical resonators into the quantum realm [3], [5], [7]–[13] (see [14] for a recent review). In addition, micro-optoelectromechanical systems (MOEMSs) are expected to play an increasing role in optical communications [15] and other photonic applications [16]–[18].

Aside from the radiation pressure, another important force that contributes to the optomechanical coupling in MOEMSs is the bolometric force [4], [19]–[25], also known as the thermal force. This force can be attributed to the heat-induced deformations of the micromechanical mirrors [23]–[26]. In general, the thermal force plays an important role in relatively large mirrors, in which the thermal relaxation rate is comparable to the mechanical resonance frequency. Phenomena such as mode cooling and self-excited oscillations [2], [20], [24], [26]–[29] have been shown in systems in which this force is dominant [4], [19], [20], [26], [30], [31].

In this paper, we investigate an optomechanical cavity having a suspended mirror in the shape of a trilayer metallic doubly clamped beam [32]–[34]. The system experimentally exhibits some unusual behaviors. For example, contrary to other experiments, in which self-excited oscillations of the mechanical resonator are optically induced when the cavity is blue detuned [35], here, the same effect occurs for the case of red-detuned cavity. Moreover, the dependence of the mechanical resonance frequency on laser power is found to be nonmonotonic [36]. These findings are attributed to optically induced thermal strain in the beam, giving rise to compressive stress that may result in buckling [37]–[42]. Bagheri *et al.* [43] have recently reported the utilization of the buckling phenomenon to develop a nonvolatile mechanical memory element in a similar optomechanical system (see also [44]).

We generalized the theoretical model that has been developed in [31] to account for the effect of buckling [45], [46]. We find that, close to buckling, the effective thermal force acting on the beam can become very large, and consequently, optomechanical coupling is greatly enhanced. Consequently, the threshold laser power needed for optically driving self-excited oscillations in the mirror can be significantly reduced. We show that the proposed theoretical model can qualitatively account for some of the experimental results. On the other hand, some other experimental observations remain elusive. For example, self-modulation of self-excited oscillations [47]–[49] is observed in some ranges of operation. Further theoretical study, which will reveal the complex structure of stability zones and bifurcations of the system [50], is needed in order to account for such findings.

II. Experimental Setup

The experimental setup (see Fig. 1) is similar to the one employed in [30]. A fiber Bragg grating (FBG) [51]–[53] and a microlens [54] are attached to the end of a single-mode fiber. The fiber can be accurately positioned using piezomotors. The system, which consists of a doubly clamped suspended multilayer micromechanical beam and the optical fiber monitoring assembly, is located inside a cryostat maintained under a typical pressure of 10^{-3} mbar and a temperature of 77 K. An optical cavity is formed between the freely suspended beam oscillating parallel to the optical axis of the cavity and either the FBG or the glass–vacuum interface at the tip of the fiber, as shown in Fig. 1(a).

The multilayer beam is fabricated by using a bulk micromachining process. A 200-nm-thick Nb layer is coated on

Manuscript received July 17, 2012; revised September 24, 2012; accepted October 18, 2012. Date of publication November 20, 2012; date of current version March 29, 2013. This work was supported in part by the German–Israeli Foundation for Scientific Research and Development under Grant 1-2038.1114.07, by the Israel Science Foundation under Grant 1380021, by the Deborah Foundation, by the Mitchell Foundation, by the Ministry of Science, by the Russell Berrie Nanotechnology Institute, by the European STREP QNEMS Project, by the MAGNET Metro 450 Consortium, and by MAFAT. Subject Editor S. Merlo.

D. Yuvaraj was with the Department of Electrical Engineering, Technion–Israel Institute of Technology, Haifa 32000, Israel. He is now with the London Centre for Nanotechnology, University College London, London, WC1H 0AH, U.K. (e-mail: yuvaraj@gmail.com).

M. B. Kadam was with the Department of Electrical Engineering, Technion–Israel Institute of Technology, Haifa 32000, Israel. He is now with Mudhoji College, Phaltan 415523, India (e-mail: kmahadeo2003@yahoo.co.in).

O. Shtempluck and E. Buks are with the Department of Electrical Engineering, Technion–Israel Institute of Technology, Haifa 32000, Israel (e-mail: shot@techunix.technion.ac.il; eyal@ee.technion.ac.il).

Color versions of one or more of the figures in this paper are available online at http://ieeexplore.ieee.org.

Digital Object Identifier 10.1109/JMEMS.2012.2226931

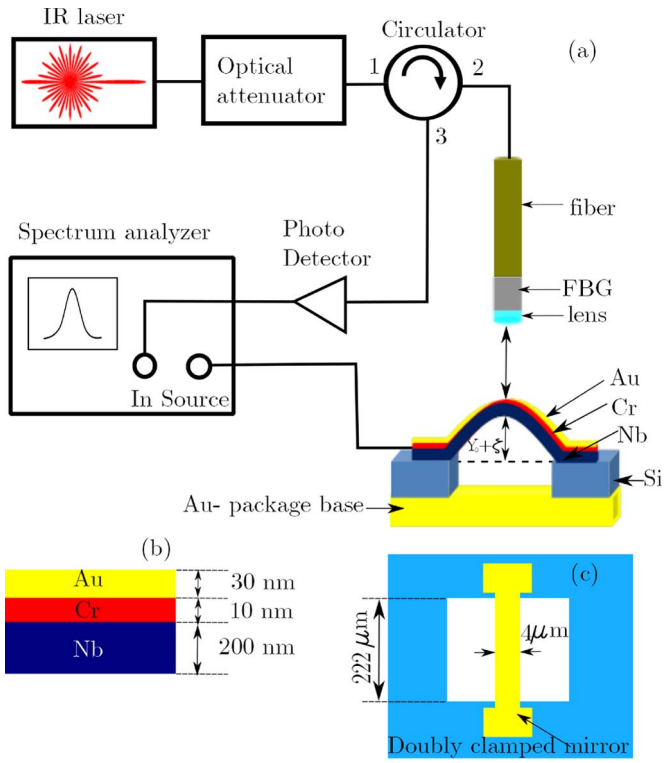

Fig. 1. Experimental setup. (a) Sample and optical displacement sensor. (b) Side-view sketch of the trilayer beam mirror. (c) Top view of suspended trilayer beam A.

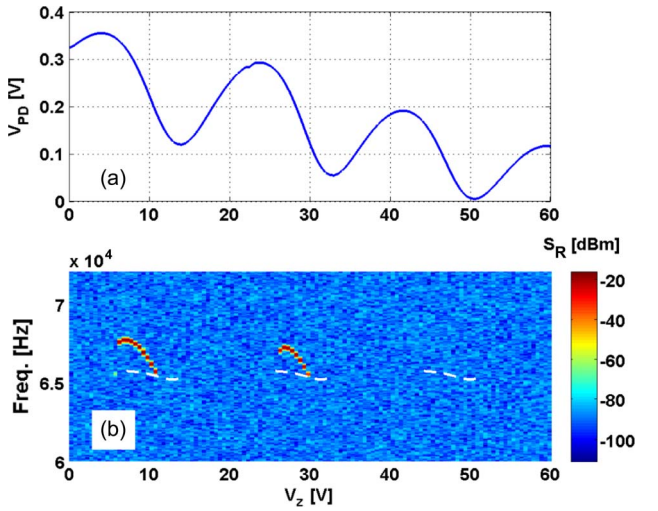

Fig. 2. Dependence on cavity length (beam A). (a) Photodetector dc voltage as a function of the voltage V_z applied to the piezomotor holding the fiber. A change of 18.5 V in V_z corresponds to a displacement of the fiber by $\lambda/2$. The laser power in this measurement is set to the value of 0.08 mW, which is lower than the threshold of self-excited oscillations. (b) Spectrum analyzer measurement of the photodetector voltage measured with a laser power of 0.16 mW. Self-excited oscillations are observed when the cavity is red detuned. The white dotted line shows the calculated value of $\Omega_{\text{eff}}/2\pi$ for the regions in V_z for which $\gamma_{\text{eff}} < 0$. The following parameters have been used for the theoretical calculation: $\theta_C = 0.06, \theta_f = 0.1, \Omega_0 = 1.2 \times 10^{-4}$, $\xi_C = 2.8 \times 10^{-3}$, $\gamma = 0.5 \times 10^{-9}$, $T_B = 0.96$, $T_A = 0.01$, $T_R = 0.6$, $\beta_Y = -1600$, and $\beta_{\text{TR}} = 2.6 \times 10^{-7}$.

prefabricated silicon nitride membranes over silicon substrates using dc magnetron sputtering at working pressure of 5.2×10^{-3} torr and argon atmosphere. Patterning on the coated substrates is done using photolithography followed by a lift-off process, in which a 10-nm-thick layer of Cr and a 30-nm-thick layer of gold–palladium $(Au_{0.85}Pd_{0.15})$ are patterned on top of the Nb layer. Front electron cyclotron resonance (ECR) plasma etching of the unmasked Nb and silicon nitride is done to suspend the AuPd/Cr/Nb multilayer beam. The process is followed by a back-side ECR plasma etching of the suspended beam to remove silicon nitride from the back side. Fig. 1(b) shows the sketch of the multilayer AuPd/Cr/Nb suspended micromechanical beam having suspended length $l = 222$ μm, width $b = 4$ μm, and total thickness $h = 240$ nm with effective Young modulus $E = 109.68 \times 10^9$ Pa, density $\rho = 9715.22$ kg/m^3, thermal expansion coefficient $\alpha = 7.76 \times 10^{-6}$ K^{-1}, and Poisson ratio $\sigma = 0.3961$. These parameters are computed by averaging over the layers using expressions taken from [33]. The top view of the suspended trilayer beam mirror that is described in the following section is shown in Fig. 1(c). We will refer to this beam hereafter as beam A.

The suspended multilayer beam can be capacitively actuated by applying voltage to it with respect to the ground plate on which the sample is mounted. The ground plate is located at 500 μm below the suspended beam. Incident optical power is controlled by attenuating the injected laser power of wavelength $\lambda \simeq 1550$ nm. The optical power reflected off the cavity is fed to a photodetector, which is monitored using a spectrum analyzer, as shown in Fig. 1(a).

III. Self-Excited Oscillations Induced by Red-Detuned Cavity

As was pointed out earlier, the optomechanical cavity under study exhibits some unusual behaviors. As is shown in Fig. 2, self-excited oscillations can be induced by a red-detuned cavity. Fig. 2(a) shows the reflected optical power versus the voltage V_z, which is applied to the piezomotor that is used to position the optical fiber along the optical axis direction. The period of oscillation in the reflected power is $\lambda/2$. In this experiment, the wavelength λ is not tuned to the reflective band formed by the FBG, and thus, the optical cavity is formed between the freely suspended beam mirror and the glass–vacuum interface at the tip of the fiber. For this case, the finesse of the cavity is much lower compared with values that can be achieved when the FBG is employed. Note that, in addition to the oscillatory part, also the averaged (over one period of oscillation) measured reflected power exhibits dependence on cavity length [see Fig. 2(a)]. The average value obtains a maximum when the cavity length coincides with the focal distance of the microlens. This occurs close to the value $V_z = 0$.

While the data shown in Fig. 2(a) are taken when the input optical power is attenuated well below the threshold of self-excited oscillations, in Fig. 2(b), in which the measured spectrum of the reflected optical signal is shown, the input power is set to 0.16 mW. Self-excited oscillations of frequency of about 67 kHz are found near $V_z = 8$ V and near $V_z = 28$ V. In both these regions where self-excited oscillations occur, the reflectivity decreases with V_z, i.e., the cavity is effectively red detuned. As was discussed earlier, the deviation from periodic dependence of the measured spectrum on cavity length with $\lambda/2$ period is attributed to the effect of the microlens.

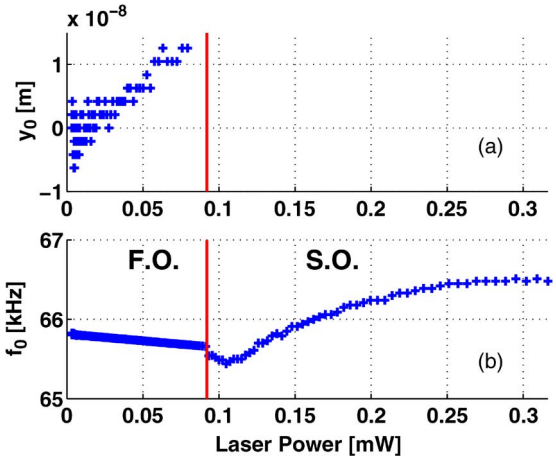

Fig. 3. Dependence of laser power (beam A). (a) Static deflection y_0. (b) Mechanical frequency f_0. The vertical red line represents the threshold of self-excited oscillations. Below the threshold, f_0 is found from the peak amplitude of forced oscillations, whereas above the threshold, f_0 is the frequency of self-excited oscillations.

The dependence on laser power P_L is shown in Fig. 3. The threshold power of self-excited oscillations occurs at 0.092 mW. In Fig. 3(a), the static position y_0 of the center of beam A is measured versus laser power below the threshold power. This is done by measuring the reflected optical power versus the voltage V_z. For each value of the laser power, this yields a plot similar to the one shown in Fig. 2(a). However, the phase of oscillations is found to depend on laser power. The value of the static deflection y_0, which is extracted from that shift in the phase, is shown in Fig. 3(a). The observed behavior indicates that the beam is deflected toward the optical fiber with increasing laser power. As will be shown in the following, this behavior indicates that the thermal force in the present case acts in the inward direction, contrary to the more common situation (e.g., for the case of radiation pressure), where cavity optomechanical forces act in the outward direction and lead to elongation of the cavity (rather than shortening as in the current case).

In Fig. 3(b), the mechanical resonance frequency f_0 is measured both below and above the threshold power of self-excited oscillations. While, below the threshold of 0.092 mW, the frequency f_0 is determined from forced oscillations (F.O.) (i.e., from the peak in the measured frequency response), above the threshold, f_0 is determined from the peak in the spectrum of self-excited oscillations (S.O.). Note the nonmonotonic dependence of f_0 on laser power. As will be argued in the following, this dependence suggests that the beam undergoes thermal buckling.

IV. Mechanical Equations of Motion

Most of the experimental findings that were presented in the previous section are not accounted by the theoretical model that has been developed in [31] (which otherwise was very successful in accounting for previous measurements in [30]). We therefore generalize the model to account for the effect of buckling in the mirror. While the derivation of the system's equations of motion is described in the Appendixes, the final equations are presented in the following in this section.

The height function $y(x,t)$ is assumed to have the shape of the first buckling configuration of a doubly clamped beam [45], [46]. Thus, for the case where the clamping points are located at $(x,y)=(\pm l/2,0)$, the height function $y(x,t)$ can be written as

$$y=\xi l\left(1+\cos\frac{2\pi x}{l}\right) \tag{1}$$

where ξ depends on time. The equation of motion for ξ, which is derived in Appendix III, is given by

$$\ddot{\xi}+2\gamma\dot{\xi}+\Omega^2\xi=F_{\rm th}+F_p e^{-i\Omega_p\tau} \tag{2}$$

where the overdot denotes a derivative with respect to the dimensionless time τ, which is related to the time t by the relation $\tau=t/\sqrt{\rho A_{\rm cs}/E}$, where ρ is the mass density, $A_{\rm cs}$ is the cross-sectional area of the beam, E is the Young modulus, γ is the dimensionless damping constant, and F_p and Ω_p are the dimensionless amplitude and angular frequency, respectively, of an externally applied force. The equation of motion (2) contains two thermo-optomechanical terms that depend on the temperature of the beam T. The first is the temperature-dependent angular resonance frequency Ω, and the second is the thermal force $F_{\rm th}$. In terms of the dimensionless temperature $\theta=(T-T_0)/T_0$, where T_0 is the temperature of the supporting substrate (i.e., the base temperature), the frequency Ω is given by $\Omega=\Omega_0\nu_C f_\nu(\theta)$, where $\Omega_0=\sqrt{\rho A_{\rm cs}/E}\omega_0$, ω_0 is the mode's angular resonance frequency, $\nu_C=\sqrt{A_{\rm cs}l^2T_0(\alpha-\alpha_s)/4\pi^2 I}$, α and α_s are the thermal expansion coefficients of the metallic beam and the substrate, respectively, I is the moment of inertia corresponding to bending in the xy plane, and the temperature dependence is expressed in terms of the dimensionless function $f_\nu(\theta)$. The dimensionless thermal force is given by $F_{\rm th}=\Omega^2\xi_C f_Y(\theta)$, where $\xi_C=\Omega_0\sqrt{3T_0(\alpha-\alpha_s)l^4/16\pi^6 I}$ and the dimensionless function $f_Y(\theta)$ represents the beam's temperature-dependent deflection. For the case of a rectangular cross section having width l_y in the y-direction and width l_z in the z-direction and for the case of bending in the xy plane, I is given by $I=l_y^3 l_z/12$. When small asymmetry is taken into account [see (23) and (25)], the functions $f_Y(\theta)$ and $f_\nu(\theta)$ can be expressed as (see Fig. 4)

$$f_Y(\theta)=\mathrm{Re}(\sqrt{\theta-\theta_C-i\theta_f}) \tag{3}$$

$$f_\nu^2(\theta)=-(\theta-\theta_C)+3f_Y^2(\theta) \tag{4}$$

where θ_C is the dimensionless buckling temperature, which is related to the buckling temperature T_C by the relation $\theta_C=(T_C-T_0)/T_0$, and where the real dimensionless constant θ_f represents the effect of asymmetry.

V. Optical Cavity

The finesse of the optical cavity is limited by loss mechanisms that give rise to optical energy leaking out of the cavity. The main escape routes are through the on-fiber mirror (FBG or glass–vacuum interface), through absorption by the metallic mirror, and through radiation; the corresponding transmission probabilities are respectively denoted by T_B, T_A, and T_R. Let

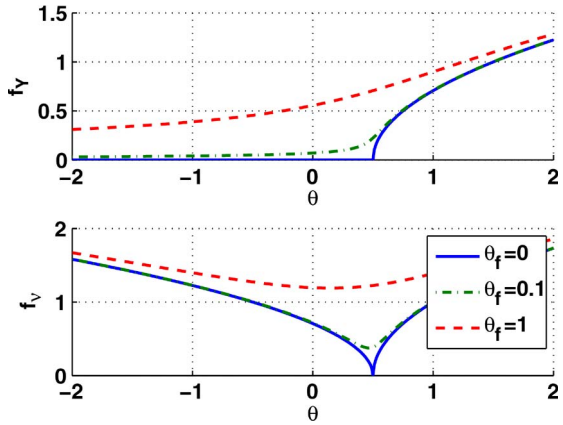

Fig. 4. Functions $f_Y(\theta)$ and $f_\nu(\theta)$ [see (3) and (4)] plotted for three different values of the asymmetry parameter θ_f and for the case where the dimensionless buckling temperature is $\theta_C = 0.5$.

y_D be the displacement of the mirror relative to a point, at which the energy stored in the optical cavity in steady state obtains a local maximum. In the ideal case, all optical properties of the cavity are periodic in y_D with a period of $\lambda/2$, where λ is the optical wavelength (although, as can be seen in Fig. 2(a), deviation from periodic behavior is experimentally observed).

It is assumed that y_D is related to ξ by the relation $4\pi y_D/\lambda = \beta_Y(\xi + \xi_f)$, where both β_Y and ξ_f are constants, which depend on the position of the fiber. For a fixed ξ, the cavity reflection probability R_C, i.e., the ratio between the reflected (outgoing) and injected (incoming) optical powers in the fiber, is given by [30]

$$R_C = \frac{\left(\frac{T_B - T_A - T_R}{2}\right)^2 + 2\left[1 - \cos\left(\beta_Y(\xi + \xi_f)\right)\right]}{\left(\frac{T_B + T_A + T_R}{2}\right)^2 + 2\left[1 - \cos\left(\beta_Y(\xi + \xi_f)\right)\right]}. \quad (5)$$

The heating power Q due to optical absorption of the suspended micromechanical mirror can be expressed as $Q = I(\xi)P_L$, where P_L is the power of the monochromatic laser light incident on the cavity and where the function $I(\xi)$ is given by [30]

$$I(\xi) = \frac{T_B T_A}{\left(\frac{T_B + T_A + T_R}{2}\right)^2 + 2\left[1 - \cos\left(\beta_Y(\xi + \xi_f)\right)\right]}. \quad (6)$$

VI. Thermal Balance Equation

The temperature T evolves according to the following thermal balance equation:

$$\frac{dT}{dt} = \frac{Q}{C} - \frac{H(T - T_0)}{C} \quad (7)$$

where C is the heat capacity, H is the thermal transfer coefficient, and Q is the heating power due to optical absorption. In terms of the dimensionless temperature θ and the dimensionless time τ, the thermal balance equation becomes

$$\dot{\theta} = \beta_P I(\xi) - \beta_{\mathrm{TR}}\theta \quad (8)$$

where $\beta_{\mathrm{TR}} = \sqrt{\Upsilon/E}H/C$ is the dimensionless thermal rate and $\beta_P = \sqrt{\Upsilon/E}P_L/CT_0$ is the dimensionless injected laser power.

VII. Small-Amplitude Limit

The coupling between the equation of motion for ξ (2) and the one for θ (8) originates from three terms, namely, the θ-dependent frequency Ω, the θ-dependent force F_{th} (i.e., the thermal force) [see (2)], and the ξ-dependent optical heating power [the term $I(\xi)$ in (8)]. The case where the first two coupling terms are linearized (i.e., approximated by a linear function of θ) is identical to the case that was studied in [31], in which slow-envelope evolution equations for the system were derived, and the amplitudes and the corresponding oscillation frequencies of different limit cycles were analyzed. By employing the same analysis (and the same simplifying assumptions) for the present case, one finds that the coupling leads to renormalization of the mechanical damping rate, which effectively becomes

$$\gamma_{\mathrm{eff}} = \gamma + \frac{f'_Y I' \xi_C \beta_P}{2\left(1 + \frac{\beta_{\mathrm{TR}}^2}{\Omega^2}\right)} \quad (9)$$

where $I' = dI/d\xi$ and $f'_Y = df_Y/d\theta$. The corresponding effective mechanical resonance frequency Ω_{eff} is given by

$$\Omega_{\mathrm{eff}} = \Omega - \frac{(\gamma_{\mathrm{eff}} - \gamma)\beta_{\mathrm{TR}}}{\Omega_p}. \quad (10)$$

The white dotted line in Fig. 2(b) shows the calculated value of Ω_{eff} [see (10)] for the regions in V_z for which $\gamma_{\mathrm{eff}} < 0$ [see (9)]. The system's parameters that were used for the calculation are listed in the caption of Fig. 2. Note that (9) and (10), which were derived by assuming the limit of small amplitudes, become inapplicable in most of the region, in which self-excited oscillations are observed in Fig. 2(b), and consequently, relatively large deviation between data and the prediction of (10) is expected.

The threshold of instability, i.e., Hopf bifurcation, occurs when γ_{eff} vanishes. For the case where the dominant coupling mechanism between the mechanical resonator and the optical field arises due to radiation pressure, instability can occur only for the so-called case of blue detuning, i.e., the case where $I' < 0$. However, contrary to the case of radiation pressure [35], [55], which always acts in the outward direction, the thermal force due to buckling can act in both directions. We refer to the case where $f'_Y > 0$ as the case of outward buckling, in which, due to buckling, the optical cavity becomes longer, whereas the opposite case of inward buckling occurs when $f'_Y < 0$. As can be seen from (9), the threshold laser power β_P at which Hopf bifurcation occurs is inversely proportional to $|f'_Y|$. Close to the buckling temperature θ_C and when asymmetry is small (i.e., when $|\theta_f| \ll 1$), the factor $|f'_Y|$ can become very large [see (3) and Fig. 4], and consequently, the threshold laser power in that region can become very small.

VIII. High Laser Power

Other interesting effects have been observed with relatively high laser power. Two examples are presented in the following. The multilayer beam mirror that was used for the experiments that are introduced in this section (see Figs. 5 and 6) has the

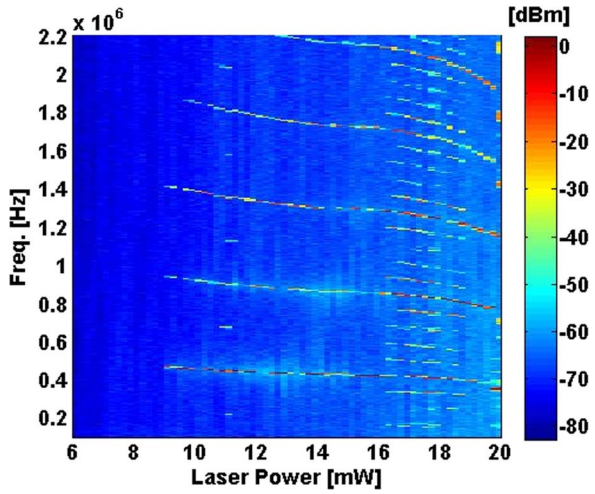

Fig. 5. In addition to the harmonics in the measured spectrum due to self-excited oscillations of mode 1 of beam B, subharmonics of order 1/2 and order 1/5 are observed.

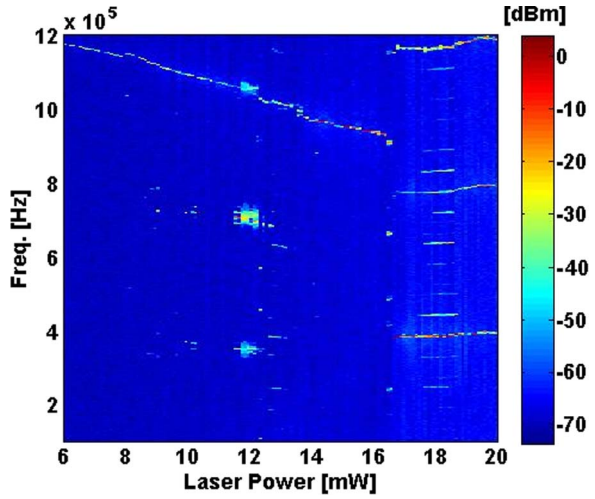

Fig. 6. Subharmonics of order 1/3 near input power of 11.9 mW are attributed to excitation of mode 1 by the self-oscillating mode 2, which has a frequency f_2 that is three times larger than f_1 in that region.

same layer structure as beam A [see Fig. 1(b)]; however, its length is $l = 120\ \mu$m, and its width is $b = 20\ \mu$m. We will refer to this beam hereafter as beam B. The same fabrication process has been employed for both beams. The two lowest lying modes of bean B, which are hereafter referred to as mode 1 and mode 2, have resonance frequencies f_1 and f_2 of about 510 and 1200 kHz, respectively (note that these values vary with laser power and cavity length).

The self-excited oscillations of mode 1 are shown in Fig. 5. In this measurement, the sample is kept grounded, and the reflected optical power is measured using a spectrum analyzer as a function of input optical power. In the frequency window that has been employed for this measurement, the first five harmonics of the self-oscillating mode 1 are seen. In addition, for some values of input power, the spectrum contains subharmonics. Close to input power of 11 mW, the subharmonics indicate that period doubling occurs, whereas in the range of 16.2–18.6 mW, the period is multiplied by a factor of five. While the period doubling effect has been predicted for a similar system by Blocher *et al.* [50], the underlying mechanism responsible for the period multiplication by a factor of five is yet undetermined.

The data in Fig. 6, which were taken with a modified cavity length, exhibit self-excited oscillations of mode 2 in the laser input power range of 6–16.5 mW. Above that range, self-excited oscillations of mode 1 are observed. Near input power of 11.9 mW, the ratio between f_2 and f_1 is three, i.e., $f_2 = 3f_1$. This gives rise to strong intermode coupling, which leads to excitation of mode 1 by the self-oscillating mode 2, as can be seen from the subharmonics of order 1/3 that are measured in that range.

Note that, for other cavity lengths, the measured spectrum of reflected power can exhibit wideband response when the input laser power is sufficiently large. This possibly indicates that the dynamics becomes chaotic [50].

IX. Conclusion

In summary, an optomechanical cavity having a buckled mirror may exhibit some unusual behaviors when the operating temperature is close to the buckling temperature. In that range, the instability threshold can be reached with relatively low laser power. Moreover, contrary to the more common case, the instability is obtained with red detuned laser light for the case of inward buckling. With relatively high laser power, other interesting effects are observed in the unstable region, including period doubling and intermode coupling. Further theoretical work is needed to account for such effects.

Appendix I
Lagrangian

Consider a beam made of a material having mass density ρ and Young modulus E. In the absence of tension, the length of the beam is l_0. The beam is doubly clamped to a substrate at the points $(x, y) = (\pm l/2, 0)$, and the motion of the beam's axis, which is described by the height function $y(x, t)$, is assumed to be exclusively in the xy plane. The corresponding moment of inertia is denoted by I. The Lagrangian functional L is given by [46]

$$L = \int_{-l/2}^{\frac{l}{2}} dx\, L_d - \frac{\beta_A E l}{8}\left(\int_{-l/2}^{\frac{l}{2}} dx \left(\frac{\partial y}{\partial x}\right)^2\right)^2 \tag{11}$$

where

$$L_d = \frac{A_{\rm cs}\rho}{2}\left(\frac{\partial y}{\partial t}\right)^2 - \frac{N}{2}\left(\frac{\partial y}{\partial x}\right)^2 - \frac{EI}{2}\left(\frac{\partial^2 y}{\partial x^2}\right)^2 + fy \tag{12}$$

is the Lagrangian density, $A_{\rm cs}$ is the cross-sectional area of the beam, f is the externally applied force per unit length, and

$$N = EA_{\rm cs}\frac{l - l_0}{l_0} \tag{13}$$

is the tension in the beam for the straight case where $y = 0$. The beam's equation of motion is found from the principle of least

action to be given by [45]

$$\Upsilon\frac{\partial^2 y}{\partial t^2}=\left(N+\frac{A_{\rm cs}E}{2l}\int\limits_{-l/2}^{\frac{l}{2}}dx\left(\frac{\partial y}{\partial x}\right)^2\right)\frac{\partial^2 y}{\partial x^2}-EI\frac{\partial^4 y}{\partial x^4}+f \tag{14}$$

where $\Upsilon=\rho A_{\rm cs}$ is the mass density per unit length.

Appendix II
First Buckling Configuration

Consider the case where the deflection $y(x,t)$ has the shape of the first buckling configuration [45], i.e., $y=A_y l(1+\cos(2\pi x/l))$, where A_y is a dimensionless time-dependent amplitude. In order to account for a possible asymmetry, the force f is allowed to be a nonzero constant [42], [46]. The Lagrangian (11) for the present case becomes

$$L_0=\frac{3\beta_A\rho l^5\left(\frac{dA_y}{dt}\right)^2}{4}-\pi^2 NlA_y^2-4\pi^4\beta_I El^3A_y^2+fl^2A_y-\frac{\pi^4\beta_A El^3A_y^4}{2} \tag{15}$$

where $\beta_A=A_{\rm cs}/l^2$ and $\beta_I=I/l^4$. Alternatively, L_0 can be expressed as

$$L_0=T_0-U_0 \tag{16}$$

where the kinetic energy T_0 is given by

$$T_0=\frac{m_0l^2\left(\frac{dA_y}{dt}\right)^2}{2} \tag{17}$$

with $m_0=3\beta_A\rho l^3/2$ and where the potential energy U_0 is given by

$$U_0=\frac{m_0\omega_0^2l^2}{2}u(A_y) \tag{18}$$

where

$$u(A_y)=\eta_1A_y+\eta_2A_y^2+\eta_4A_y^4 \tag{19}$$

$\eta_1=-2f/m_0\omega_0^2$, $\eta_2=1-\beta_{L_d}$, $\eta_4=\pi^4\beta_A El/m_0\omega_0^2$, $\beta_{L_d}=-N/4\pi^2\beta_I El^2$, and $\omega_0^2=(2\pi)^4\beta_I E/3\rho A_{\rm cs}$.

Local minimum points A_{y0} of the potential U_0 are found by solving $0=du/dA_y$. The dimensionless potential $u(A_y)$ can be expanded near one of its local minimum points A_{y0} to second order in $A_y-A_{y0}\equiv\xi$ as $u=u_0+\nu^2\xi^2+O(\xi^3)$, where both u_0 and $\nu=\sqrt{\eta_2+6\eta_4A_{y0}^2}$ are constants.

For the case where $\eta_1=0$, the coordinate A_{y0} is given by $A_{y0}=\pm{\rm Re}\sqrt{-\eta_2/2\eta_4}$. The solution for the case of small $|\eta_1|$ can be approximated by

$$A_{y0}={\rm Re}\sqrt{-\frac{\eta_2+i\left(4\eta_1^2\eta_4\right)^{1/3}}{2\eta_4}} \tag{20}$$

provided that $|\eta_2|$ is small, i.e., provided that the system is close to buckling conditions. The corresponding approximation for ν is found from the relation $\nu=\sqrt{\eta_2+6\eta_4A_{y0}^2}$.

Appendix III
Mechanical Equation of Motion

Let α and α_s be the thermal expansion coefficients of the metallic beam and the substrate, respectively. At some given temperature $T_{\rm TF}$, the tension N is assumed to vanish. Since the substrate is much larger than the beam, one may assume that the substrate thermally contracts (or expands) as if the suspended beam was not attached to it, namely, the distance between both clamping points at temperature $T=T_{\rm TF}+\Delta_T$ becomes $l_s=l_0(1+\alpha_s\Delta_T)$, where l_0 is the distance at the tension-free temperature $T_{\rm TF}$. The tension N needed to keep the beam clamped to the substrate is thus given by $N=EA_{\rm cs}(\alpha_s-\alpha)\Delta_T$ [56]. Thus, the dimensionless parameter β_{L_d} can be expressed as a function of the dimensionless temperature

$$\theta=\frac{T-T_0}{T_0} \tag{21}$$

where T_0 is the temperature of the supporting substrate (i.e., the base temperature), as $\beta_{L_d}=\beta_A\beta_{T0}(\theta+\beta_{\rm TF})/4\pi^2\beta_I$, where $\beta_{T0}=T_0(\alpha-\alpha_s)$ and $\beta_{\rm TF}=(T_0-T_{\rm TF})/T_0$. Alternatively, β_{L_d} can be expressed as

$$\beta_{L_d}=1+\frac{\beta_A\beta_{T0}(\theta-\theta_C)}{4\pi^2\beta_I} \tag{22}$$

where $\theta_C=4\pi^2\beta_I/\beta_A\beta_{T0}-\beta_{\rm TF}$ is the dimensionless temperature at which buckling occurs in the symmetric case (i.e., the case where $\eta_1=0$).

With the help of (22), the parameters A_{y0} and ν can be expressed as functions of the dimensionless temperature θ. For the case of small asymmetry, one has [see (20)]

$$A_{y0}=\xi_C f_Y(\theta) \tag{23}$$

where the function $f_Y(\theta)$ is given by (22), $\theta_f=4\pi^2\beta_I(4\eta_1^2\eta_4)^{1/3}/\beta_A\beta_{T0}$, and the coefficient ξ_C is given by

$$\xi_C=\sqrt{\frac{\beta_A\beta_{T0}}{8\pi^2\beta_I\eta_4}}=\sqrt{\frac{3T_0(\alpha-\alpha_s)A_{\rm cs}\rho l^4\omega_0^2}{16\pi^6EI}}. \tag{24}$$

The corresponding approximation for ν is given by

$$\nu=\nu_C f_\nu(\theta) \tag{25}$$

where

$$\nu_C=\sqrt{\frac{\beta_A\beta_{T0}}{4\pi^2\beta_I}}=\sqrt{\frac{A_{\rm cs}l^2T_0(\alpha-\alpha_s)}{4\pi^2I}} \tag{26}$$

and the function $f_\nu(\theta)$ is given by (4). The functions $f_Y(\theta)$ and $f_\nu(\theta)$ are plotted in Fig. 4.

The temperature dependence of A_{y0} can be taken into account by adding a thermal force term $F_{\rm th}$ [37], [57], [58] to the equation of motion of the mechanical amplitude $\xi=A_y-A_{y0}$. Similarly, the temperature dependence of ν can be taken into

account by including a thermal frequency shift term. When, in addition, damping and external driving are taken into account, the equation of motion (2) for ξ is obtained.

ACKNOWLEDGMENT

The authors would like to thank Y. Starosvetsky for the many fruitful discussions and important comments. D. Yuvaraj and M. B. Kadam have equally contributed to this paper.

REFERENCES

[1] V. B. Braginsky and A. B. Manukin, "Ponderomotive effects of electromagnetic radiation," (in Russian), *ZhETF (J. Experiment. Theor. Phys.)*, vol. 52, pp. 986–989, 1967.

[2] K. Hane and K. Suzuki, "Self-excited vibration of a self-supporting thin film caused by laser irradiation," *Sens. Actuators A, Phys.*, vol. 51, no. 2/3, pp. 179–182, Feb. 1996.

[3] S. Gigan, H. R. Böhm, M. Paternostro, F. Blaser, J. B. Hertzberg, K. C. Schwab, D. Bauerle, M. Aspelmeyer, and A. Zeilinger, "Self cooling of a micromirror by radiation pressure," *Nature*, vol. 444, no. 7115, pp. 67–70, Nov. 2006.

[4] C. H. Metzger and K. Karrai, "Cavity cooling of a microlever," *Nature*, vol. 432, no. 7020, pp. 1002–1005, Dec. 2004.

[5] T. J. Kippenberg and K. J. Vahala, "Cavity optomechanics: Back-action at the mesoscale," *Science*, vol. 321, no. 5893, pp. 1172–1176, Aug. 2008.

[6] C. Metzger, I. Favero, S. Camerer, D. Konig, H. Lorenz, J. P. Kotthaus, and K. Karrai, "Optical cooling of a micromirror of wavelength size," *Appl. Phys. Lett.*, vol. 90, no. 10, p. 104101, Mar. 2007.

[7] H. J. Kimble, Y. Levin, A. B. Matsko, K. S. Thorne, and S. P. Vyatchanin, "Conversion of conventional gravitational-wave interferometers into quantum nondemolition interferometers by modifying their input and/or output optics," *Phys. Rev. D, Part. Fields*, vol. 65, no. 2, p. 022002, Dec. 2001.

[8] T. Carmon, H. Rokhsari, L. Yang, T. J. Kippenberg, and K. J. Vahala, "Temporal behavior of radiation-pressure-induced vibrations of an optical microcavity phonon mode," *Phys. Rev. Lett.*, vol. 94, no. 22, p. 223902, Jun. 2005.

[9] O. Arcizet, P.-F. Cohadon, T. Briant, M. Pinard, and A. Heidmann, "Radiation-pressure cooling and optomechanical instability of a micromirror," *Nature*, vol. 444, no. 7115, pp. 71–74, Nov. 2006.

[10] A. M. Jayich, J. C. Sankey, B. M. Zwickl, C. Yang, J. D. Thompson, S. M. Girvin, A. A. Clerk, F. Marquardt, and J. G. E. Harris, "Dispersive optomechanics: A membrane inside a cavity," *New J. Phys.*, vol. 10, no. 9, p. 095008, Sep. 2008.

[11] A. Schliesser, R. Riviere, G. Anetsberger, O. Arcizet, and T. J. Kippenberg, "Resolved-sideband cooling of a micromechanical oscillator," *Nat. Phys.*, vol. 4, no. 5, pp. 415–419, May 2008.

[12] C. Genes, D. Vitali, P. Tombesi, S. Gigan, and M. Aspelmeyer, "Ground-state cooling of a micromechanical oscillator: Comparing cold damping and cavity-assisted cooling schemes," *Phys. Rev. A, Atom. Mol. Opt. Phys.*, vol. 77, no. 3, p. 033804, Mar. 2008.

[13] J. D. Teufel, D. Li, M. S. Allman, K. Cicak, A. J. Sirois, J. D. Whittaker, and R. W. Simmonds, "Circuit cavity electromechanics in the strong coupling regime," *Nature*, vol. 471, no. 7337, pp. 204–208, Mar. 2011.

[14] M. Poot and H. S. J. van der Zant, "Mechanical systems in the quantum regime," *Phys. Rep.*, vol. 511, no. 5, pp. 273–335, Feb. 2012.

[15] M. C. Wu, O. Solgaard, and J. E. Ford, "Optical MEMS for lightwave communication," *J. Lightwave Technol.*, vol. 24, no. 12, pp. 4433–4454, Dec. 2006.

[16] N. A. D. Stokes, R. M. A. Fatah, and S. Venkatesh, "Self-excitation in fibre-optic microresonator sensors," *Sens. Actuators A, Phys.*, vol. 21, no. 1–3, pp. 369–372, Feb. 1990.

[17] S. E. Lyshevski and M. A. Lyshevski, "Nano- and microoptoelectromechanical systems and nanoscale active optics," in *Proc. 3rd IEEE Conf. Nanotechnol.*, Aug. 2003, vol. 2, pp. 840–843.

[18] M. Hossein-Zadeh and K. J. Vahala, "An optomechanical oscillator on a silicon chip," *IEEE J. Sel. Top. Quantum Electron.*, vol. 16, no. 1, pp. 276–287, Jan./Feb. 2010.

[19] G. Jourdan, F. Comin, and J. Chevrier, "Mechanical mode dependence of bolometric backaction in an atomic force microscopy microlever," *Phys. Rev. Lett.*, vol. 101, no. 13, p. 133904, Sep. 2008.

[20] C. Metzger, M. Ludwig, C. Neuenhahn, A. Ortlieb, I. Favero, K. Karrai, and F. Marquardt, "Self-induced oscillations in an optomechanical system driven by bolometric backaction," *Phys. Rev. Lett.*, vol. 101, no. 13, p. 133903, Sep. 2008.

[21] F. Marino and F. Marin, "Chaotically spiking attractors in suspended mirror optical cavities," *Phys. Rev. E, Stat., Nonlin., Soft Matter Phys.*, vol. 83, no. 1, p. 015202, Jan. 2010.

[22] J. Restrepo, J. Gabelli, C. Ciuti, and I. Favero, "Classical and quantum theory of photothermal cavity cooling of a mechanical oscillator," *Compt. Rendus Phys.*, vol. 12, no. 9/10, pp. 860–870, Dec. 2011.

[23] S. D. Liberato, N. Lambert, and F. Nori, "Quantum limit of photothermal cooling," *Phys. Rev. A, Atom., Mol., Opt. Phys.*, vol. 83, no. 3, p. 033809, Mar. 2010.

[24] F. Marquardt, J. G. E. Harris, and S. M. Girvin, "Dynamical multistability induced by radiation pressure in high-finesse micromechanical optical cavities," *Phys. Rev. Lett.*, vol. 96, no. 10, p. 103901, Mar. 2006.

[25] M. Paternostro, S. Gigan, M. S. Kim, F. Blaser, H. R. Böhm, and M. Aspelmeyer, "Reconstructing the dynamics of a movable mirror in a detuned optical cavity," *New J. Phys.*, vol. 8, no. 6, pp. 107–108, Jun. 2006.

[26] K. Aubin, M. Zalalutdinov, T. Alan, R. B. Reichenbach, R. Rand, A. Zehnder, J. Parpia, and H. Craighead, "Limit cycle oscillations in CW laser-driven NEMS," *J. Microelectromech. Syst.*, vol. 13, no. 6, pp. 1018–1026, Dec. 2004.

[27] K. Kim and S. Lee, "Self-oscillation mode induced in an atomic force microscope cantilever," *J. Appl. Phys.*, vol. 91, no. 6, pp. 4715–4719, Apr. 2002.

[28] T. Corbitt, D. Ottaway, E. Innerhofer, J. Pelc, and N. Mavalvala, "Measurement of radiation-pressure-induced optomechanical dynamics in a suspended Fabry–Perot cavity," *Phys. Rev. A, Atom., Mol., Opt. Phys.*, vol. 74, no. 2, p. 21802, Aug. 2006.

[29] T. Carmon and K. J. Vahala, "Modal spectroscopy of optoexcited vibrations of a micron-scale on-chip resonator at greater than 1 GHz frequency," *Phys. Rev. Lett.*, vol. 98, no. 12, p. 123901, Mar. 2007.

[30] S. Zaitsev, A. K. Pandey, O. Shtempluck, and E. Buks, "Forced and self-excited oscillations of optomechanical cavity," *Phys. Rev. E, Stat., Nonlin., Soft Matter Phys.*, vol. 84, no. 4, p. 046605, Oct. 2011.

[31] O. Gottlieb, S. Zaitsev, and E. Buks, "Nonlinear dynamics of a microelectromechanical mirror in an optical resonance cavity," *Nonlinear Dyn.*, vol. 69, no. 4, pp. 1589–1610, Sep. 2012.

[32] A. Michael and C. Y. Kwok, "Buckling shape of elastically constrained multi-layered micro-bridges," *Sens. Actuators A, Phys.*, vol. 135, no. 2, pp. 870–880, Apr. 2007.

[33] D. S. Ross, A. Cabal, D. Trauernicht, and J. Lebens, "Temperature-dependent vibrations of bilayer microbeams," *Sens. Actuators A, Phys.*, vol. 119, no. 2, pp. 537–543, Apr. 2005.

[34] W. Riethmuller and W. Benecke, "Thermally excited silicon microactuators," *IEEE Trans. Electron Devices*, vol. 35, no. 6, pp. 758–763, Jun. 1988.

[35] D. A. Rodrigues and A. D. Armour, "Amplitude noise suppression in cavity-driven oscillations of a mechanical resonator," *Phys. Rev. Lett.*, vol. 104, no. 5, p. 053601, Feb. 2010.

[36] H. Okamoto, T. Kamada, K. Onomitsu, I. Mahboob, and H. Yamaguchi, "Optical tuning of coupled micromechanical resonators," *Appl. Phys. Exp.*, vol. 2, no. 6, p. 062202, Jun. 2009.

[37] W. Fang and J. A. Wickert, "Post buckling of micromachined beams," *J. Micromech. Microeng.*, vol. 4, no. 3, pp. 116–122, Sep. 1994.

[38] D. W. Coffin and F. Bloom, "Elastica solution for the hygrothermal buckling of a beam," *Int. J. Non-Lin. Mech.*, vol. 34, no. 5, pp. 935–947, Sep. 1999.

[39] J. M. Gere and S. P. Timoshenko, *Mechanics of Materials*. Boston, MA: PWS-Kent, 1997.

[40] J. J. Talghader, "Thermal and mechanical phenomena in micromechanical optics," *J. Phys. D, Appl. Phys.*, vol. 37, no. 10, pp. R109–R122, May 2004.

[41] A. Ettouhami, A. Essaid, N. Ouakrim, L. Michel, and M. Limou.D, "Thermal buckling of silicon capacitive pressure sensor," *Sens. Actuators A, Phys.*, vol. 57, no. 3, pp. 167–171, Dec. 1996.

[42] M. McCarthy, N. Tiliakos, V. Modi, and L. G. Frechette, "Thermal buckling of eccentric microfabricated nickel beams as temperature regulated nonlinear actuators for flow control," *Sens. Actuators A, Phys.*, vol. 134, no. 1, pp. 37–46, Feb. 2007.

[43] M. Bagheri, M. Poot, M. Li, W. P. H. Pernice, and H. X. Tang, "Dynamic manipulation of nanomechanical resonators in the high-amplitude regime and non-volatile mechanical memory operation," *Nat. Nanotechnol.*, vol. 6, no. 11, pp. 726–732, Nov. 2011.

[44] D. Roodenburg, J. W. Spronck, H. S. J. van der Zant, and W. J. Venstra, "Buckling beam micromechanical memory with on-chip readout," *Appl. Phys. Lett.*, vol. 94, no. 18, p. 183501, May 2009.

[45] A. H. Nayfeh, W. Kreider, and T. J. Anderson, "Investigation of natural frequencies and mode shapes of buckled beams," *AIAA J.*, vol. 33, no. 6, pp. 1121–1126, Jun. 1995.
[46] W. E. Lawrence, M. N. Wybourne, and S. M. Carr, "Compressional mode softening and Euler buckling patterns in mesoscopic beams," *New J. Phys.*, vol. 8, no. 10, p. 223, Oct. 2006.
[47] M. Pandey, K. Aubin, M. Zalalutdinov, R. B. Reichenbach, A. T. Zehnder, R. H. Rand, and H. G. Craighead, "Analysis of frequency locking in optically driven MEMS resonators," *J. Microelectromech. Syst.*, vol. 15, no. 6, pp. 1546–1554, Dec. 2006.
[48] M. Pandey, R. Rand, and A. Zehnder, "Perturbation analysis of entrainment in a micromechanical limit cycle oscillator," *Commun. Nonlin. Sci. Numer. Simul.*, vol. 12, no. 7, pp. 1291–1301, Oct. 2007.
[49] M. Pandey, R. H. Rand, and A. T. Zehnder, "Frequency locking in a forced Mathieu–van der Pol–Duffing system," in *Proc. ASME Conf.*, 2007, vol. 2007, pp. 893–903.
[50] D. Blocher, A. T. Zehnder, R. H. Rand, and S. Mukerji, "Anchor deformations drive limit cycle oscillations in interferometrically transduced MEMS beams," *Finite Elem. Anal. Design*, vol. 49, no. 1, pp. 52–57, Feb. 2012.
[51] A. W. Snyder and J. D. Love, *Optical Waveguide Theory*. New York: Springer-Verlag, 1983.
[52] A. W. Snyder and J. D. Love, *Optical Waveguide Theory*. London, U.K.: Chapman & Hall, 1983.
[53] L. Poladian, "Resonance mode expansions and exact solutions for nonuniform gratings," *Phys. Rev. E, Stat., Nonlin., Soft Matter Phys.*, vol. 54, no. 3, pp. 2963–2975, Sep. 1996.
[54] Y. Mao, S. Chang, S. Sherif, and C. Flueraru, "Graded-index fiber lens proposed for ultrasmall probes used in biomedical imaging," *Appl. Opt.*, vol. 46, no. 23, pp. 5887–5894, Aug. 2007.
[55] A. Schliesser, P. Del'Haye, N. Nooshi, K. J. Vahala, and T. J. Kippenberg, "Radiation pressure cooling of a micromechanical oscillator using dynamical backaction," *Phys. Rev. Lett.*, vol. 97, no. 24, p. 243905, Dec. 2006.
[56] A. K. Pandey, O. Gottlieb, O. Shtempluck, and E. Buks, "Performance of an AuPd micromechanical resonator as a temperature sensor," *Appl. Phys. Lett.*, vol. 96, no. 20, p. 203105, May 2010.
[57] W. Fang and J. A. Wickert, "Determining mean and gradient residual stresses in thin films using micromachined cantilevers," *J. Micromech. Microeng.*, vol. 6, no. 3, pp. 301–309, Sep. 1996.
[58] T. G. Leong, B. R. Benson, E. K. Call, and D. H. Gracias, "Thin film stress driven self-folding of microstructured containers," *Small*, vol. 4, no. 10, pp. 1605–1609, Oct. 2008.

D. Yuvaraj received the Ph.D. degree from the Indian Institute of Science, Bangalore, India, in 2010.

From 2010 to 2012, he was a Postdoctoral Fellow with the Quantum Electronics Laboratory, Technion—Israel Institute of Technology, Haifa, Israel. He is currently in the pursuit of Majorana fermions in the semiconductor–superconductor interface at the London Centre for Nanotechnology, University College London, London, U.K. His research interests include integration of nanomaterials by nanofabrication for applications in nanoelectronics and integrated devices.

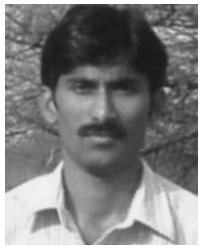

M. B. Kadam received the M.Sc. and Ph.D. degrees in physics from Shivaji University, Kolhapur, India.

He was a Viterbi Postdoctoral Fellow with the Quantum Engineering Laboratory, Technion–Israel Institute of Technology, Haifa, Israel. He is currently an Assistant Professor of physics with Mudhoji College, Phaltan, India. His current research involves SQUID-coupled nanoelectromechanical systems, quantum optics, superconductivity, and material science.

Dr. Kadam was awarded with a Council of Scientific and Industrial Research (New Delhi) Senior Research Fellowship.

Oleg Shtempluck was born in Moldova in 1949. He received the M.Sc. degree in electronic engineering from the Physical Department, Chernivtsi State University, Chernivtsi, Ukraine (former Soviet Union), in 1978.

He was a Team Leader with the Division of Design Engineering, Electronmash, from 1983 to 1992 and a Stamp and Mold Design Engineer with Ikar Company from 1992 to 1999, both in Ukraine. He is currently a Laboratory Engineer with the Microelectronics Research Center, Technion—Israel Institute of Technology, Haifa, Israel. His research concerns semiconductors and dielectrics.

Eyal Buks received the B.Sc. degree in mathematics and physics from Tel Aviv University, Tel Aviv, Israel, in 1991 and the M.Sc. and Ph.D. degrees in physics from the Weizmann Institute of Science, Rehovot, Israel, in 1994 and 1998, respectively. His graduate work concentrated on interference and dephasing in mesoscopic systems.

From 1998 to 2002, he was a Postdoctoral Scholar with the California Institute of Technology (Caltech), Pasadena, studying experimentally nanomachining devices. He is currently an Associate Professor with the Technion—Israel Institute of Technology, Haifa, Israel. His current research is focused on nanomachining and mesoscopic physics.